

# Can Cosmic Shear Shed Light on Low Cosmic Microwave Background Multipoles?

Michael Kesden, Marc Kamionkowski, and Asantha Cooray  
Mail Code 130-33, California Institute of Technology, Pasadena, California 91125  
(June 2003)

The lowest multipole moments of the cosmic microwave background (CMB) are smaller than expected for a scale-invariant power spectrum. One possible explanation is a cutoff in the primordial power spectrum below a comoving scale of  $k_c \simeq 5.0 \times 10^{-4} \text{ Mpc}^{-1}$ . This would affect not only the CMB but also the cosmic-shear (CS) distortion of the CMB. Such a cutoff increases significantly the cross-correlation between the large-angle CMB and cosmic-shear patterns. The cross-correlation may be detectable at  $> 2\sigma$  which, when combined with the low CMB moments, may tilt the balance between a  $2\sigma$  result and a firm detection of a large-scale power-spectrum cutoff. As an aside, we also note that the cutoff increases the large-angle cross-correlation between the CMB and low-redshift tracers of the mass distribution.

One of the more intriguing results to come from the Wilkinson Microwave Anisotropy Probe (WMAP) [1] is confirmation of the absence of large-scale temperature correlations in the cosmic microwave background (CMB), or equivalently, a suppression of power in the quadrupole and octupole moments, found earlier by the Cosmic Background Explorer [2]. A variety of measures of the power spectrum—from the  $l = 4$  moment of the CMB power spectrum, which probes wavelengths  $\sim 10^4 \text{ Mpc}$ , to galaxy surveys and the Lyman-alpha forest, which probe down to 1–10 Mpc—show consistency with a scale-invariant spectrum of primordial perturbations. Thus, the suppression of the  $l = 2$  and  $l = 3$  moments of the CMB power spectrum come as a bit of a surprise.

Is this simply a statistical fluke? Or is something novel occurring just beyond our observable cosmological horizon? Possibilities include remnants of a pre-inflationary Universe, a curvature scale just larger than the horizon, and/or exotic inflation [3,4]. If there is indeed a suppression of large-scale power, it occurs at distance scales  $\sim 10^4 \text{ Mpc}$  [4], larger than those typically probed by galaxy surveys. Future experiments to determine the lowest moments of the CMB power spectrum are also of limited value because current measurements are already dominated by cosmic variance rather than instrumental noise. Thus, although the current evidence for new super-horizon physics is tantalizing, the prospects for further testing it are limited.

In this paper we point out that there exists another probe of the mass distribution on these largest distance scales. Cosmic shear (CS), weak gravitational lensing by density perturbations along the line of sight, will produce identifiable distortions in the temperature-polarization pattern of the CMB. When observed, these distortions map the gravitational potential projected along a given line of sight. Here we show that a power-spectrum cutoff enhances significantly (roughly a factor of four) the cross-correlation between the CMB and CS distortion of the CMB on the largest scales. This cross-correlation may be detectable at the  $> 2\sigma$  level and may thus pro-

vide a valuable cross-check to the current  $\sim 2\sigma$  evidence for a dearth of large-scale CMB power. As an aside, we also show that the large-angle cross-correlation between the CMB and low-redshift tracers of large-scale structure [5] is roughly doubled if the large-scale cutoff is real. Although recent detections [6] of this effect are at smaller scales than would be affected by a large-scale cutoff, correlations on larger scales might be probed by future experiments.

Below we first discuss the large-scale CS power spectra, as well as the cross-correlation of the CS pattern with the CMB temperature pattern. We then construct an estimator for the cross-correlation, and show that it can distinguish the cross-correlation with and without a cutoff at roughly the  $2\sigma$  level. When combined with the already suspiciously low  $l = 2$  and  $l = 3$  moments of the CMB power spectrum, this finding may tilt the balance between a  $2\sigma$  result and a  $3\sigma$  discrepancy with scale invariance.

Perturbations in the matter density induce perturbations to the gravitational potential  $\Phi(\mathbf{r}, z)$  which then induce temperature perturbations in the CMB through the Sachs-Wolfe effect

$$\Theta(\hat{\mathbf{n}}) = \frac{1}{3}\Phi(\mathbf{r}_0, z_0) - 2 \int_0^{r_0} \frac{d\Phi}{dr}(\mathbf{r}, z(r)) dr, \quad (1)$$

where  $\mathbf{r}$  and  $z$  are the physical comoving distance and redshift, respectively, and the subscript 0 denotes these quantities at the last-scattering surface. The position vector  $\mathbf{r}$  points in the direction  $\hat{\mathbf{n}}$  on the sky. The potential at redshift  $z$  can be related to its present-day value with the linear-theory growth factor  $G(z)$  (normalized to unity today) through  $\Phi(\mathbf{r}, z) = (1+z)G(z)\Phi(\mathbf{r}, 0)$ . The first term in Eq. (1) comes from density perturbations at the surface of last scatter, while the second term (the integrated Sachs-Wolfe effect; ISW) comes from density perturbations along the line of sight.

Relating the potential to the matter perturbation through the Poisson equation, if the three-dimensional matter power spectrum is  $P(k)$  as a function of wavenum-

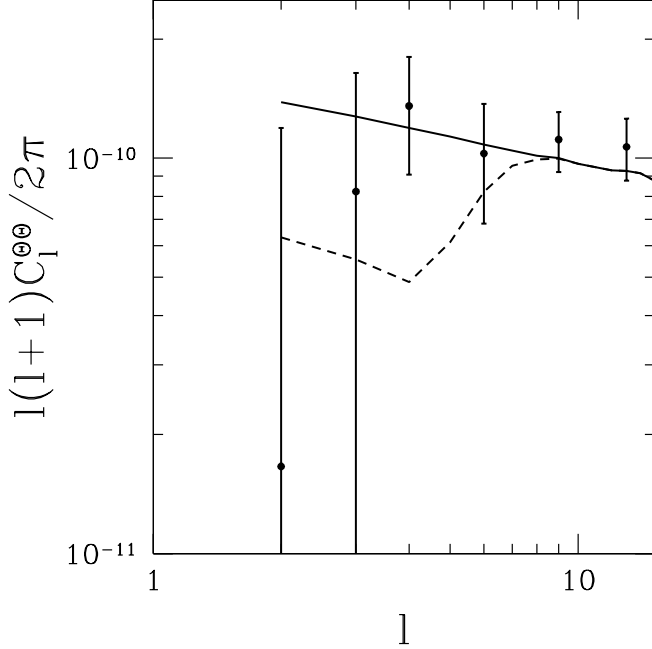


FIG. 1. The CMB temperature power spectrum. The solid curve is the power spectrum of Eq. (2) for the ISW effect without a cutoff. The dashed curve has a cutoff in  $P(k)$  below  $k_c = 5.0 \times 10^{-4} \text{ Mpc}^{-1}$ . The binned error bars represent actual WMAP data.

ber  $k$ , then the angular power spectrum for temperature fluctuations is

$$C_l^{\Theta\Theta} \propto \int dk k^{-2} P(k) [\tilde{\Theta}_l(k)]^2, \quad (2)$$

as a function of multipole moment  $l$ , where

$$\begin{aligned} \tilde{\Theta}_l(k) = & \frac{1}{3}(1+z_0)G(z_0)j_l(kr_0) \\ & - 2 \int_0^{z_0} dz [(1+z)G(z)]' j_l(kr(z)), \end{aligned} \quad (3)$$

and the prime denotes derivative with respect to redshift  $z$ . The main contributions to the integral in Eq. (2) come from wavenumbers  $k$  near  $10^{-4} \text{ Mpc}^{-1}$  (see, e.g., Fig. 7 in Ref. [7]).

If scale invariance holds out to super-horizon scales (as predicted by the generic inflationary model), then the power spectrum  $P(k)$  at distance scales relevant for  $l \lesssim 10$  is simply  $P(k) \propto k^n$ , with  $n$  near unity. This is certainly what the CMB data show at multipole moments  $l \geq 4$  and it is consistent with determinations of the power spectrum from the CMB and large-scale structure out to scales as small as  $\sim$ few Mpc. Thus, the observed suppression of  $C_2^{\Theta\Theta}$  and  $C_3^{\Theta\Theta}$  shown in Fig. 1 is a bit of a surprise.

The same potential perturbations  $\Phi(\mathbf{r}, z)$  that contribute to the Sachs-Wolfe effect also give rise to weak

gravitational lensing described by the projected potential,

$$\phi(\hat{\mathbf{n}}) = -2 \int_0^{r_0} dr \frac{r_0 - r}{r_0 r} \Phi(\mathbf{r}, z(r)). \quad (4)$$

The angular power spectrum of the lensing potential is then

$$C_l^{\phi\phi} \propto \int dk k^{-2} P(k) [\tilde{\phi}_l(k)]^2. \quad (5)$$

In fact, the only difference between this expression and its SW counterpart is the replacement of  $\tilde{\Theta}_l(k)$  by

$$\tilde{\phi}_l(k) = -2 \int_0^{z_0} \frac{cdz}{H(z)} \frac{r_0 - r(z)}{r_0 r(z)} (1+z)G(z)j_l(kr(z)). \quad (6)$$

The projected potential receives contributions from a wide variety of distances, peaked at roughly half the comoving distance to the surface of last scatter. The lowest multipole moments of the CS power spectrum come from wavenumbers  $k$  near  $10^{-4} \text{ Mpc}^{-1}$ . Since the small- $k$  Fourier modes of the potential that give rise to low- $l$  CS moments are the same as those that give rise to the low- $l$  CMB moments, we anticipate that the CS power spectrum should also reflect the suppression of large-scale power. Evaluating these expressions numerically, however, we find that the cutoff suppresses  $C_2^{\phi\phi}$  by no more than  $\sim 10\%$ , too small to be detected.

However, the CMB and CS multipole moments are generated by the same underlying potential fluctuations, and so there should be some cross-correlation between the two. And as we show, this cross-correlation turns out to be increased significantly if there is a cutoff. The cross-correlation power spectrum  $C_l^{\Theta\phi}$  is

$$C_l^{\Theta\phi} \propto \int dk k^{-2} P(k) \tilde{\Theta}_l(k) \tilde{\phi}_l(k). \quad (7)$$

We can define a dimensionless cross-correlation coefficient,  $r_l \equiv (C_l^{\Theta\phi})^2 / C_l^{\Theta\Theta} C_l^{\phi\phi}$ . If  $\tilde{\Theta}_l(k)$  and  $\tilde{\phi}_l(k)$  had precisely the same  $k$  dependence, then the CMB maps would be maximally correlated,  $r_l = 1$ . In this case, we would be able to predict precisely that the CS spherical-harmonic coefficients should be  $\phi_{lm} = (C_l^{\Theta\phi} / C_l^{\Theta\Theta}) \Theta_{lm}$  in terms of the measured temperature coefficients  $\Theta_{lm}$ . Moreover, if  $r_l$  were equal to unity, then a CS map might be used to confirm the CMB measurements, but it would add no additional statistically-independent information on the large-scale power spectrum.

If, on the other hand, there was no overlap between  $\tilde{\Theta}_l(k)$  and  $\tilde{\phi}_l(k)$  whatsoever, then there would be no cross-correlation,  $r_l = 0$ . In this case, the CS pattern could not confirm the CMB measurement, but it would provide a statistically independent probe of the large-scale power spectrum.

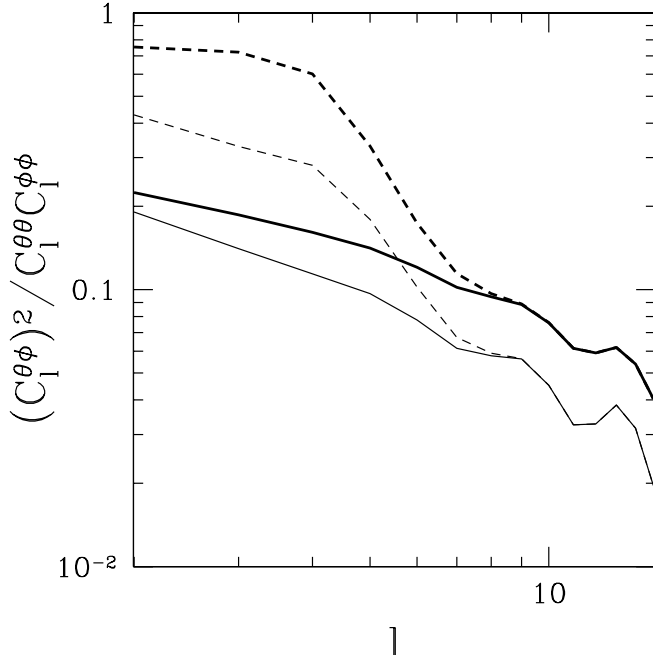


FIG. 2. The dimensionless correlation  $(C_l^{\theta\phi})^2/C_l^{\theta\theta}C_l^{\phi\phi}$  between maps of the CMB temperature and lensing potential. The solid curve shows this correlation in the absence of a cutoff, while the dashed curve is for a cutoff  $k_c = 5.0 \times 10^{-4} \text{ Mpc}^{-1}$ . The upper, darker curves correspond to the lensing potential seen by sources at the CMB last-scattering surface, while the lower, lighter curves correspond to lensing sources at redshift  $z = 1.0$ .

Most generally,  $0 < r_l < 1$ , and the lensing spherical-harmonic coefficients will be

$$\phi_{lm} = (C_l^{\theta\phi}/C_l^{\theta\theta})\Theta_{lm} + [C_l^{\phi\phi} - (C_l^{\theta\phi})^2/C_l^{\theta\theta}]^{1/2} \zeta, \quad (8)$$

where  $\zeta$  is a Gaussian random variable with zero mean and unit variance; i.e., there is a correlated part determined by the CMB pattern and an uncorrelated part.

Fig. 2 shows our central result: the cross-correlation coefficient for a scale-invariant spectrum and one in which  $P(k) = 0$  for  $k < k_c = 5 \times 10^{-4} \text{ Mpc}^{-1}$ . The dramatic increase in the cross-correlation for the lowest  $l$  in the presence of a cutoff can be understood by examining the two terms of Eq. (1). The first of these terms, generated at the last-scattering surface, is uncorrelated with the lensing potential; the second term is a line-of-sight integral like the projected potential of Eq. (4). Since the contribution of the first term comes from a larger distance from the observer than that of the second term, correspondingly larger structures with lower wavenumber  $k$  will be projected onto the angular scale set by the multipole moment  $l$ . The lowest multipole moments will correspond to structures at the last-scattering surface with  $k < k_c$ , implying that in the presence of a cutoff only

the second term of Eq. (1) will be nonvanishing for the lowest multipole moments. Since it is only this term that is correlated to the lensing potential, the dimensionless cross-correlation will be significantly higher in the presence of a cutoff. It is important to note that this increase in the dimensionless cross-correlation in the presence of a cutoff is an independent prediction and not merely a consequence of the observed suppression of  $C_l^{\theta\theta}$  for low  $l$ . If the CMB and CS multipole moments  $\Theta_{lm}$  and  $\phi_{lm}$  were multiplied by an  $l$ -dependent normalization to suppress power on large scales,  $r_l$  itself would remain unaffected because it is dimensionless. The independence of this prediction allows estimates of  $r_l$  from CMB and CS maps to constrain  $k_c$  with greater statistical significance than measurements of  $C_l^{\theta\theta}$  alone.

We now determine how well measurements of  $r_l$  can discriminate between a model with a scale-invariant power spectrum and one with a cutoff (i.e.,  $P(k) = 0$  for  $k < k_c = 5.0 \times 10^{-4} \text{ Mpc}^{-1}$ ). Higher-order correlations in a high-resolution low-noise CMB temperature-polarization map, can be used to construct estimators [8] for the projected potential and thus estimators  $\hat{C}_l^{\theta\phi}$  and  $\hat{C}_l^{\phi\phi}$ , in addition to those  $\hat{C}_l^{\theta\theta}$  for the temperature obtained already by WMAP. An estimator  $\hat{r}_l \equiv (\hat{C}_l^{\theta\phi})^2/\hat{C}_l^{\theta\theta}\hat{C}_l^{\phi\phi}$  for  $r_l$  can then be formed. Although it is not an unbiased estimator, it is sensitive to  $r_l$  and converges to  $r_l$  for  $l \gg 1$ . For a given realization of the CMB and CS patterns,  $r_l$  can be estimated independently for each value of  $l$ . We have calculated the probability distributions for  $\hat{r}_l$  for each  $l$  from many different Monte Carlo realizations of the two models for  $r_l$  described above. The CMB coefficients  $\Theta_{lm}$  are set to the values consistent with the WMAP power spectrum shown in Fig. 1, while the uncorrelated part of  $\phi_{lm}$  is determined for each realization of the two models in accordance with Eq. (8). We assume the CS projected potential is reconstructed from a full-sky CMB temperature-polarization map with  $7'$  angular resolution and noise-equivalent temperature of  $0.46 \mu\text{K}\sqrt{\text{sec}}$ . The different predictions for  $\hat{r}_3$  for the two models are shown in Fig. 3; the predictions for  $\hat{r}_2$  and  $\hat{r}_4$  are qualitatively similar while for  $\hat{r}_5$  the two probability distributions begin to merge and for  $\hat{r}_6$  they are almost indistinguishable.

Assuming that the first model (no cutoff) is correct, we calculated the fraction of realizations in which the measured values of  $\hat{r}_l$  would lead us to conclude that they were more likely drawn from the probability distributions of the second model. This occurs only 0.7% of the time, implying that only 0.7% of the time would cosmic variance mislead us into thinking that a cutoff as large as  $k_c = 5.0 \times 10^{-4} \text{ Mpc}^{-1}$  was favored over the no-cutoff model. Since the CMB coefficients  $\Theta_{lm}$  are constrained to a single realization consistent with WMAP in both models, this measurement would be statistically independent of the low observed CMB multipole moments

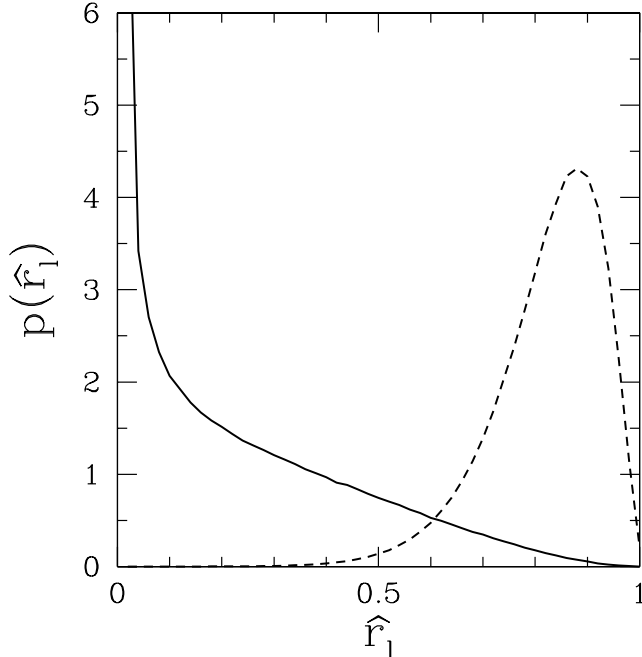


FIG. 3. Probability distributions for  $\hat{r}_l$  for  $l = 3$  for the two models described in the text; the solid curve corresponds to the model without a cutoff in  $P(k)$  while the dashed curve has a cutoff  $k_c = 5.0 \times 10^{-4} \text{ Mpc}^{-1}$ .

themselves for the purpose of distinguishing the two models. It could thus increase the  $\sim 2\sigma$  discrepancy of that measurement into a  $> 3\sigma$  detection of a large-scale cutoff in the power spectrum.

Finally, we consider the cross-correlation between the CMB and low-redshift ( $z \lesssim 1$ ) tracers of large-scale structure [5] that several groups have already claimed to detect [6]. To estimate the effect of a cutoff, we have calculated the cross-correlation between the CMB and CS of a hypothetical population of sources at redshift  $z = 1$  for models with and without a cutoff. As indicated by the lighter curves in Fig. 2, a cutoff boosts the cross-correlation coefficient for these low-redshift sources by roughly a factor of two. Similar results are obtained for cross-correlation with the galaxy distribution. Although recent detections of the cross-correlation occur at smaller scales ( $l \simeq 30$ ) than those effected by the cutoff, future large-scale surveys could be sensitive to a cutoff-induced enhancement.

The WMAP observations clearly support the  $\Lambda$ CDM concordance model, but they do present a few tantalizing discrepancies. Perhaps the most intriguing is the sharp decrease in observed power at the lowest multipole moments shown in Fig. 1. A variety of fundamental causes for this large-scale suppression can be modeled empirically by an effective cutoff  $k_c$  in the primordial power spectrum  $P(k)$ . Though the WMAP team found that only 0.15% of simulated CMB maps had less

power on large scales [1], it would be highly desirable to find corroborating evidence to confirm that this observation is not merely a statistical anomaly. One possibility is measurements of the polarization signal from nearby galaxy clusters, which are proportional to their local CMB quadrupole moment [9]. We have proposed here that the cross-correlation  $C_l^{\Theta\phi}$  could provide additional evidence. Although the experimental requirements for measurements of the CS distortions to the CMB are ambitious, they are closely aligned with those for the CMBPOL experiment that appears in NASA's roadmap. Thus, this measurement, like the effect it seeks to study, is on the horizon.

## ACKNOWLEDGMENTS

This work was supported in part by NASA NAG5-11985 and DoE DE-FG03-92-ER40701. Kesden acknowledges the support of an NSF Graduate Fellowship.

- 
- [1] C. L. Bennett et al., astro-ph/0302207; D. N. Spergel et al., astro-ph/0302209.
  - [2] C. L. Bennett et al., *Astrophys. J. Lett.* **464**, L1 (1996).
  - [3] G. Efstathiou, astro-ph/0303127; A. Blanchard et al., astro-ph/0304237; B. Feng and X. Zhang, astro-ph/0305020; M. Kawasaki and F. Takahashi, hep-ph/0305319; S. DeDeo, R. R. Caldwell, and P. J. Steinhardt, *Phys. Rev. D* **67**, 103509 (2003).
  - [4] C. R. Contaldi et al., astro-ph/0303636; E. Gaztanaga et al., astro-ph/0304178; G. Efstathiou, astro-ph/0306431. J. M. Cline, P. Crotty, and J. Lesgourgues, astro-ph/0304558.
  - [5] R. G. Crittenden and N. Turok, *Phys. Rev. Lett.* **76**, 575 (1996); M. Kamionkowski, *Phys. Rev. D* **54**, 4169 (1996); S. P. Boughn, R. G. Crittenden, and N. G. Turok, *New Astron.* **3**, 275 (1998); A. Kinkhabwala and M. Kamionkowski, *Phys. Rev. Lett.* **82**, 4172 (1999); U. Seljak and M. Zaldarriaga, *Phys. Rev. D* **60**, 043504 (1999).
  - [6] S. P. Boughn and R. G. Crittenden, astro-ph/0305001; M. R.olta et al., astro-ph/0305097; P. Fosalba, E. Gaztanaga, and F. Castander, astro-ph/0307533; P. Fosalba and E. Gaztanaga, astro-ph/0305468; R. Scranton et al. (SDSS Collaboration), astro-ph/0307335; N. Afshordi, Y. Loh, and M. Strauss, astro-ph/0308260.
  - [7] M. Kamionkowski and D. N. Spergel, *Astrophys. J.* **432**, 7 (1994).
  - [8] U. Seljak and M. Zaldarriaga, *Phys. Rev. Lett.* **82**, 2636 (1999); W. Hu, *Phys. Rev. D* **64**, 083005 (2001); W. Hu, *Astrophys. J. Lett.* **557**, L79 (2001); W. Hu and T. Okamoto, *Astrophys. J.* **574**, 566 (2002); M. Kesden, A. Cooray, and M. Kamionkowski, *Phys. Rev. Lett.* **89**, 011304 (2002); L. Knox and Y.-S. Song, *Phys. Rev. Lett.* **89**, 011303; M. Kesden, A. Cooray, and M. Kamionkowski,

Phys. Rev. D **67**, 123507 (2003); C. Hirata and U. Seljak, astro-ph/0306354.

- [9] A. Cooray and D. Baumann, Phys. Rev. D **67**, 063505 (2003); M. Kamionkowski and A. Loeb, Phys. Rev. D **56**, 4511 (1997).